

Astroblastoma: Immunohistochemical and ultrastructural study of distinctive epithelial and probable tanycytic differentiation

メタデータ	言語: English 出版者: 公開日: 2008-12-15 キーワード (Ja): キーワード (En): 作成者: KUBOTA, Toshihiko, SATO, Kazufumi, ARISHIMA, Hidetaka, TAKEUCHI, Hiroaki, KITAI, Ryuhei, NAKAGAWA, Takao メールアドレス: 所属:
URL	http://hdl.handle.net/10098/1809

Case Report

Astroblastoma : Distinctive Epithelial and Probable Tanycytic Differentiation : Immunohistochemical and Ultrastructural Study

**Toshihiko Kubota, M.D., Ph D., Kazufumi Sato M.D., Ph.D.,
Hidetaka Arishima, M.D., Ph.D., Hiroaki Takeuchi M.D., Ph.D.,
Ryuhei Kitai, MD., Ph.D., Takao Nakagawa, M.D., Ph.D.,**

Department of Neurosurgery, Faculty of Medical Sciences, University of
Fukui

23-3 Shimoaizuki, Matsuoka-Cho, Yoshida-Gun, Fukui
910-1193, JAPAN

Address correspondence to : Toshihiko Kubota, M.D.
Department of Neurosurgery, Faculty of Medical Sciences, University of
Fukui

23-3 Shimoaizuki, Mastuoka-Cho, Yoshida-Gun, Fukui
910-1193, JAPAN
TEL: +81-776-61-8384, FAX: +81-776-61-8115
E-mail: tkubott@fmsrsa.fukui-med.ac.jp

We report the clinicopathological findings of astroblastoma found in an 8-year-old girl who was subsequently treated for 11 years. The primary superficially circumscribed tumor was located in the fronto-parietal lobe, while the recurrent and the second recurrent tumor were restricted to the same region 11 years later. The tumors obtained on these three occasions showed fundamentally the same histological, immunohistochemical and fine structural features. They exhibited astrocytic as well as ependymal tanycytic features with apparent epithelial cell lineage. The tumor cells showed typical features of astroblastoma comprising prominent perivascular pseudorosettes with remarkable vascular sclerosis. The immunohistochemical study revealed intensive positivity of glial fibrillary acidic protein (GFAP), vimentin, epithelial membrane antigen (EMA), cytokeratin, connexin 26 and 32, desmocollin1 and neuronal cadherin. The fine structure revealed divergent types of junctional complexes, some of which were connected with tonofilament bundles. Numerous microvilli protruded and basal lamina abutted on the tumor cell surface. We report these unique histological features, and stress that astroblastoma should be categorized as a specific type of neuroepithelial tumor.

Keywords : astroblastoma, tanycyte, cytokeratin, desmosome, microvilli

INTRODUCTION

Bailey and Cushing coined the name “astroblastoma” for one type of glial tumor¹⁾, and it is classified into neuroepithelial tumors of uncertain origin in the 2000 WHO classification²⁾. Bonnin and Rubinstein described clinicopathological study of a series of 23 cases and concluded that the pure type of astroblastoma, in which almost all of the tumor tissue is characterized by a radiating perivascular arrangement, rarely exists³⁾. Recent case reports of astroblastoma showed that the tumors were predominantly localized in the superficial cerebral hemisphere in a circumscribed fashion in young adults, and that some cases survived for a long time⁴⁻¹⁹⁾.

In 1989, Rubinstein and Herman proposed an intriguing new idea about the origin of astroblastoma based on their vigorous investigations²⁰⁾. They studied long term tissue- and organ-cultures of two cases by electron microscopy and immunohistochemistry. They found that the fine structural characteristics observed both in the original tumor and in vitro were those of intermediate-type astrocytes and ependymocytes. These tumor cells recapitulated the structure of ependymal tanycytes, a precursor cell which is normally found along the ependymal lining of the embryonal and mammalian brain, but is distinct from the epithelial ependymal cell. After Rubinstein’s study, there have been no further detailed immuno-histochemical and ultrastructural studies concerning astroblastoma.

We report a case in which astroblastoma showed probable tanycytic differentiation with apparent epithelial cell type of immunohistochemical and ultrastructural features.

PATIENT AND METHODS

Patient

An 8-year-old girl complained of mild headache, and subsequently her consciousness level gradually deteriorated during 2 days, and right motor weakness developed. She was referred to our hospital after she consulted a neurosurgeon who diagnosed her illness as a brain mass by evaluating the magnetic resonance imaging(MRI) on 23th of October 1993. On admission, her consciousness level was drowsy, even though she was able

to have rapport with other persons. Her right extremities showed increased tonus and motor weakness. Plain computerized tomography (CT) demonstrated a large high-density hematomatous mass in the left fronto-parietal lobe with surrounding edema (Fig.1A). Contrast enhanced T1-weighted MRI revealed a heterogenously enhanced large circumscribed round mass with peritumoral edema (Fig.1B). The surface of the mass contacted the dura, and it imaged as an extraaxial tumor. The left cerebral hemisphere was remarkably swollen, and a midline shift to the right was seen. The left carotid angiography demonstrated a faint tumor stain.

The patient underwent a fronto-parietal craniotomy on 26th October 1993. The surface of the cerebral cortex exhibited a contused hemorrhage-like appearance. Part of the mass was confirmed to consist of a gliomatous tissue with hemorrhage by examination of the biopsy specimen. The mass was bloody, pinkish gray, easily aspirated, and of soft consistency. The tumor margin was moderately well circumscribed and the tumor was macroscopically totally removed. The Ki-67 labeling index was high (15.6 %). The patient was given conventional LINAC radiotherapy of 30 Gy to the whole brain and 20 Gy to the tumor-originating area. She was also treated with an anticancer drug (an alkylating agent, nimustine hydrochloride =ACNU, 20~30mg) via the left internal carotid artery catheterization from November 1993 to July 1997(45 months), with 2- to 6-month intervals. She was well and had no neurological deficits after her discharge, and went to school without intellectual problems. Follow-up MRI was performed 3 times per year after the tumor resection. No recurrent tumor was detected through late 2002(Fig.1C).

A tiny, 5-mm diameter, enhanced recurrent lesion was eventually found on 8th of February 2003. The recurrent tumor grew to 15 mm in diameter (Fig1D) as of 29th of October 2003. She was admitted again to remove the lesion. Frontal craniotomy was performed and a superficially circumscribed soft, pinkish gray tumor was totally removed on 11th November 2003. The histological diagnosis of the recurrent tumor was the same as that of the initial tumor, astroblastoma. The patient was followed by MRI every 2 months without chemotherapy or radiotherapy. A second recurrent tumor developed 4 months after the second operation in the same region, and was macroscopically totally removed on 13th April 2004. This tumor was also recurrent astroblastoma. She was given 40 Gy stereotactic radiotherapy after the third operation, and she later returned to regular work.

Pathological examination

Representative surgical specimens obtained at the three operations were examined by light and electron microscopy. For the light microscopic studies, the specimens were fixed in 10 % formalin and 70 % alcohol solution, embedded in paraffin and stained with hematoxylin and eosin.

For immunohistochemical examination, staining was performed using the En Vision+ technique (DAKO) or the catalyzed signal amplification (CSA) system (DAKO) on 2 μ m-thick consecutive sections. For epitope retrieval, specimens were pretreated with 0.1% protease or with microwaves (400W, 2x5 min). Primary antibodies against glial fibrillary acidic protein (GFAP), vimentin, keratin(56 & 64Kd), cytokeratin(8 & 18Kd), epithelial membrane antigen (EMA), neurofilament²¹⁾, connexin 26, connexin 32, connexin 43, desmocollin-1, desmoglein-2, desmocollin-3, epithelial cadherin (E-cadherin), neuronal cadherin(N-cadherin) and Ki-67 were used at appropriate dilutions (Table 1). Immunopositive and negative control stainings were always performed.

For ultrastructural studies, representative specimens were fixed immediately in 2.5% glutaraldehyde, postfixed in 2 % osmium tetroxide, and embedded in Epon-Araldite mixture. Ultrathin sections were stained with uranyl acetate followed by lead citrate, and were examined with a Hitachi H-7000 electron microscope.

RESULTS

Light microscopy

The surgical specimens from the primary, the first recurrent and the second recurrent tumor showed essentially the same histological pattern, with dominant perivascular pseudorosettes (Fig.2A~D). The majority of the tumor cells comprised perivascular pseudorosettes (Fig. 2 A), and some vessel walls showed remarkable hyaline thickening (Fig.2B). The histological diagnosis was a typical astroblastoma. The tumor margin was usually smooth and circumscribed (Fig.2A). The lesion mainly consisted of the clustering of tumor cells around the blood vessels, resulting in the figures of perivascular pseudorosettes in cross-sections (Fig2A~C), and a ribbon-like quality in longitudinal-sections (Fig.2D). The short cytoplasmic cell processes that radiated from the vessels were broad and not markedly tapered. The nuclei contained compact chromatin, were round, and showed infrequent mitosis. Compactly arranged non-papillary tumor areas were

also frequently seen. Large hemorrhagic lesions were observed in the primary tumor. The vessel walls in the primary tumor frequently showed prominent hyaline thickening (Fig.2B), but not these in the recurrent ones. These recurrent tumor showed signs of a malignant nature, with nuclear atypia, mitoses and a wide necrotic area. Endothelial cell proliferation was not seen. The intercellular spacing between the pseudorosettes was often wide (Fig2A, D).

Immunohistochemistry

The majority of tumor cells were strongly positive for GFAP (Fig.2E) and vimentin. Epithelial cell markers such as keratin(56 & 64Kd), cytokeratin(8 & 18Kd) and EMA were focally positive in the primary tumor, and more frequently positive in the recurrent tumors(**Table 2**). Keratin(56 & 64Kd) was focally stained in the cytoplasm of tumor cells, while cytokeratin(8 & 18KD) was evenly and intensively stained (Fig.2F). EMA immunopositivity showed a tendency to be localized at the cytoplasmic margin (Fig.2G). Some cell adhesion molecules showed various degrees of staining. Connexin(Cx) 26(Fig.2H) and Cx32 were remarkably positive in the spaces between the tumor cells, but Cx43 was negative. Desmocollin 1 was strongly positive between the tumor cells (Fig.2I), although both desmoglein 2 and desmocollin 3 were negative. E-cadherin was weakly positive, while N-cadherin was moderately to strongly positive around the outer membrane of the tumor cells (Fig.2J). Ki-67 labeling indices of the primary tumor, the first recurrent and the second recurrent tumors were 15.6%, 25% and 26.4%, respectively.

Electron microscopy

The fine structural examination revealed irregular-shaped cytoplasm in the tumor cells. The cells were connected with each other by well-developed junctional complexes (Fig.3, Fig.4, Fig.5). These cell junctions showed various different features. Some desmosomes projected tonofilament bundles (Fig3), others showed immature junctional complexes (Fig.4B) or completed features of desmosomes (Fig.5A). Moreover, irregularly developed desmosomes with tonofilament bundles were frequently seen (Fig.5B). The cells usually contained well-developed cytoplasmic organelles such as rough endoplasmic reticulum, free ribosomes and mitochondria (Fig.3, 4B). Among these organelles, perinuclear tonofilament bundles were clearly seen (Fig.3). On the other

hand, intermediate filaments fully occupied the cytoplasm (Fig.4A). Nuclei showed polygonal, round or irregular shape, and prominent nucleoli (Fig. 3, 4). Some tumor cells exhibited abundant microvillous projections (Fig.4B). The apical surface of the tumor cells projected closely packed microvilli which fanned out from a narrow base resulting in a “purse-string appearance”(Fig.6A). Conspicuous closely spaced microvilli resembling ependymal microrosettes were rarely observed (Fig.6B). Cilia were never found, although they are frequently seen in ependymoma. Basal lamina often abutted on the free margin of the cytoplasmic membrane of the tumor cells.

DISCUSSION

Clinicopathological features

Astroblastoma is not accepted by some neuropathologists as a specific clinicopathological entity²⁾. Diagnostic skepticism has dogged this tumor since its category was adopted in the brain tumor classification by Bailey and Cushing in 1926¹⁾. After their proposal, three large astroblastoma series delineating unique clinicopathologic features for differentiating astroblastoma from other similiar histologic glial neoplasms have been reported^{3,14,22)}. Until recently, only a few other case reports have been sporadically described, and astroblastomas were believed to be a specific type of neoplasm characterized by their clinicopathological features. Accurate epidemiological data about astroblastomas is not available²⁾. They occur rarely occasion, frequently affect younger patients, and commonly show a circumscribed, supratentorial superficially located mass. Our case described here is compatible with the aforementioned classification of astroblastoma. The tumor was superficially circumscribed in the fronto-parietal lobe of a young girl.

Histologically, the tumor was composed of astroblastic vascular pseudorosettes and frequent prominent sclerotic vascular walls. Brat et al. proposed that the perivascular processes of astroblastomas are not fibrillar, nor do they show stromal fibrillarity¹⁴⁾. This lack of fibrillarity is an essential feature in distinguishing astroblastoma from other glial neoplasms, as seen in our case. Additionally, Brat et al.¹⁴⁾ and Bonnin and Rubinstein³⁾ stressed that astroblastoma contained marked vascular sclerosis that ranged in extent. Severe vascular sclerosis was observed in our primary tumor. The tumor border was well circumscribed, and it was clear that the tumor was expanding its peripheral part and was rather sharply demarcated from the

surrounding parenchymal tissue.

Recent advanced neuroimaging methods revealed specific figures of astroblastoma. Port et al. reported that astroblastomas were generally circumscribed, cystic and solid lesions on MRI¹⁶⁾. These lesions have relatively little peritumoral T2 hyperintensity for their large size, which suggests a lack of local tumor infiltration into the surrounding brain tissue. Such imaging characteristics can assist in differentiating astroblastomas from other brain tumors. On the other hand, in a large series of astroblastomas, the histologically malignant type of this tumor were reported^{3,14,22)}. Such tumors showed anaplastic cells with cellular irregularity, nuclear polymorphism and focal necrosis. They resembled anaplastic astrocytoma and glioblastoma, with loss of the astroblastic nature, and resulted in short survival. Moreover, a well-differentiated astroblastoma relapsed and changed into glioblastoma and the patient died of the tumor after 4.5 years³⁾. In our case, the tumor recurred 11 years later after the first resection, and a second recurrent tumor rapidly developed 3 months later. Therefore, irradiation and chemotherapy should be considered if the Ki-67 staining index over 10 %, even the tumor shows benign histological figures¹²⁾.

Cytogenesis

The cytogenesis of astroblastomas is not known²⁾. Bailey and Cushing proposed that astroblasts are derived from the unipolar spongioblasts : their tails begin to develop processes which extend in various directions, distinguished by a broad process attached to the wall of a blood-vessel, where it becomes enlarged into what is known as the " sucker foot ", and by short stubby processes which extend in many directions from the opposite poles of the cell¹⁾. Astroblasts are embryonic cells destined to become astrocytes, more specifically, cells consisting an intermediate stage in development between spongioblasts and astrocytes. They showed that astroblasts were clearly stained by Cajal's Gold-sublimate method¹⁾.

Recent immunohistochemical findings may clarify the cytogenesis of certain brain tumors. All astroblastomas are strongly immunoreactive for GFAP and vimentin, which implies astroblastomas are astrocytic origin^{2,3,20)}. Other immunoreactive antigens such as cytokeratin and EMA were **scatteredly** stained in some astroblastoma cells^{7,14,19)}. In this study, prominent cytokeratin(8 & 18Kd), scattered keratin(56 & 64Kd) and focal EMA immunoreactivity were observed. We performed an immunohistochemical study of intracranial and spinal ependymomas in

which EMA and cytokeratin were present focally, but usually immunoreactive²³⁾. Therefore, this astroblastoma may be supposed to have come from the ependymal lineage.

We immunohistochemically investigated some cell adhesion molecules in the astroblastoma. It is well known specific cell types in the normal brain express specific types of connexin(Cx)²⁴⁾. Astrocytes express Cx43, and ependyma exhibits immunoreactivity of Cx43 and Cx26. In our study, Cx 26 and Cx32 were intensively immunopositive between the tumor cells. Combined expression of Cx26 and Cx 32 is suggested to occur in a specific cell type because this combination of Cxs and other Cx proteins was not reported in the normal brain and glioma cells. On the other hand, the absence of the Cx43 protein in our study may have be due to a reduction during tumor progression as shown crucial role of Cx43 protein down-regulation during glioma invasion²⁵⁾.

Desmocollin1 is usually found to be restricted to suprabasal layers in the epidermis as one of the desmosomal proteins²⁵⁾. Their intensive immunoreactivity of desmocollin 1 in our astroblastoma is presumed to indicate keratocytic differentiation of the tumor cells, in which abundant desmosomal junctions and tonofilaments were seen.

Cadherins are generally considered to be important regulators of morphogenesis²⁷⁾. Moreover, the down-regulation of E-cadherin expression is thought to promote tumor invasion and metastasis²⁷⁾. N-cadherin was intensively immunopositive between the tumor cells, while E-cadherin was weakly positive or negative, in our study. Recently, the down-regulation of E-cadherin expression during tumor progression has been shown to be frequently accompanied by the expression of mesenchymal cadherins such as N-cadherin²⁷⁾. Our immunohistochemical data about cadherins are presumed to indicate the so called 'cadherin switch', which is a prerequisite for tumor cell invasion and migration²⁸⁾.

Characteristic fine structures of astroblastomas have commonly been reported to reflect an astrocytic cytoplasmic nature, namely, cells are filled with intermediate filaments, and contain infrequent osmophilic inclusion bodies corresponding to Rosenthal fibers, pinocytotic vesicles, abundant glycogen granules, and scant or no microvilli, cilia or junctional complexes^{4-7,9,10,13,15,17)}. An extensive precise fine structural study in vivo and in vitro specimens of two astroblastoma cases was accomplished by Rubinstein and Herman²⁰⁾. In addition to the astrocytic ultrastructural nature, they found the following three significant new ultrastructural features : (1) closely packed microvilli mimicking a "purse-string" appearance on the free surface of the apical cells, (2) inconstant and

relatively scant intercellular junctions interrupted as microrosettes, (3) cytoplasmic pleatings, or interdigitations, over the lateral borders of the tumor cells. They stated that these fine structures are intermediary between those of astrocytes and ependymocytes. They also stressed that the tumors they described differed from typical ependymoma because of their scant junctional complexes and rare cilia. Moreover, they pointed out that these features recall the characteristic ultrastructural features of the tanycyte, i.e., marked pleating of their cell membranes²⁹⁾, thin interdigitating lamellar cytoplasmic processes²⁹⁾, and microvilli and surface blebs with a constricted pedicle²⁹⁻³¹⁾. Tanycytes were described by Horstman in 1954, who reported that ependymal basal processes penetrated into the subjacent neuropil, and that these processes often reached the pial surface and were observed to contact vascular elements along their course³²⁾. Tanycytes in adult mammals are found scattered throughout the ventricular system and circumventricular organs²⁹⁾. These areas have fenestrated capillaries and a lack of a functional blood-brain barrier, thus allowing free exchange of substances between the vascular and extracellular brain components²⁹⁾. Tanycytes are most numerous in the inferolateral walls of the third ventricle²⁹⁾. Tanycytes are also seen in the spinal cord radiating from the ependyma of the central canal to the spinal cord surface. In our case, some tumor cells exhibited a more epithelial nature, showing prominent tonofilaments with complete desmosomal structures, while others showed numerous microvilli and rarely a microrosette appearance but no cilia. Moreover, the second recurrent tumor cells projected closely compact microvilli fanning from a narrow pedicle, giving the cells a “purse-string” appearance²⁰⁾. There were sometimes numerous glial filaments in the cytoplasm. From these findings, we assume that the cytogenesis of this tumor is originated from the astrocyte lineage to ependymal cells, which are thought to have tanycytic similarities because of the numerous junctional apparatuses with microvilli and no cilia.

Interestingly, the ultrastructures of tanycytic ependymoma show well-developed junctional complexes, clusters of microvilli and abundant microfilaments^{33,34)}. These findings are closely similar to the structures observed in our case. Also, we recently reported that a chordoid glioma of the third ventricle showed a differentiated tanycytic nature, as proved by immunohistochemical and ultrastructural studies³⁵⁾. Epithelial differentiation of glial cells and ependymal cells have been described earlier, so it is not surprising to observe keratin- or tonofilament-related structures in glial tumors³⁶⁻³⁸⁾.

In conclusion, we suggest that astroblastomas are one of the

distinctive, rare tumors with a nature between that of glial and ependymal cells²⁰⁾. Precise immunohistological and ultrastructural investigations should be performed to differentiate astroblastomas from other gliomas.

ACKNOWLEDGMENTS

We are grateful to Mr Tetsuzi Hishima for his technical assistance. We also express our gratitude to Ms Kikuko Arakawa for her photographic assistance.

REFERENCES

1. Bailey P, Cushing H. *A classification of the tumors of the glioma group on a histogenetic basis with a correlated study of prognosis.*: J. B. Lippincott Company, Philadelphia, London, & Montreal, 1926; 83-84, 134-167.
2. Lantos PL, Rosenblum MK. Astroblastoma. Pathology and genetics. In : Kleihues P, Cavenee WK(ed) *Tumours of the nervous system. World Health Organization classification of tumours*. Lyon International Agency for Research on Cancer Press, 2000; 88-89.
3. Bonnin JM, Rubinstein LJ. Astroblastomas: A pathological study of 23 tumors, with a postoperative follow-up in 13 patients. *Neurosurgery* 1989; **25**: 6-13.
4. Kubota T, Hirano A, Sato K, Yamamoto S. The fine structure of astroblastoma. *Cancer* 1985; **55**: 745-750.
5. Hoag G, Sima AAF, Rozdilsky B. Astroblastoma revisited : A report of three cases. *Acta Neuropathol* 1986; **70**: 10-16.
6. Husain AN, Leestma JE. Cerebral astroblastoma: immunohistochemical and ultrastructural features. Case report. *J Neurosurg* 1986; **64**: 657-661.
7. Cabello A, Madero S, Castresana A, Diaz-Lobato R. Astroblastoma: Electron microscopy and immunohistochemical findings: Case report. *Surg Neurol* 1991; **35**: 116-121.
8. Baka JJ, Patel SC, Roebuck JR, Hearshen DO. Predominantly

- extraaxial astroblastoma: Imaging and MR spectroscopy features. *Amer J Neuroradiol* 1993; **14**: 946-950.
9. Jay V, Edwards V, Suire J, Rutka J. Astroblastoma: Report of a case with ultrastructural, cell kinetics, and cytogenetic analysis. *Pediat Pathol* 1993; **13**: 323-332.
 10. Pizer BL, Moss T, Oakhill A, Webb D, Coakham HB. Congenital astroblastoma: immunohistochemical study. Case report. *J Neurosurg* 1995; **83**: 550-555.
 11. Yuntan N, Ersahin Y, Demirtas E, Yalman O, Sener RN. Cerebral astroblastoma resembling an extra-axial neoplasm. *J Neuroradiol* 1996; **23**: 38-40.
 12. Thiessen B, Finlay J, Kulkarni R, Rosenblum MK. Astroblastoma: Does histology predict behavior? *J Neuro-Oncol* 1998; **40**: 59-65.
 13. Mierau GW, Tyson RW, McGavran L, Parker NB, Partington MD. Astroblastoma : Ultrastructural observations on a case of high-grade type. Case Report. *Ultrastruct Pathol* 1999; **23**: 325-332.
 14. Brat DJ, Hirose Y, Cohen KJ, Feuerstein BG, Burger PC. Astroblastoma: Clinicopathological features and chromosomal abnormalities defined by comparative genomic hybridization. *Brain Pathol* 2000; **10**: 342-352.
 15. Kujas M, Faillot T, Lalam T, Roncier B, Catala M, Poirier J. Astroblastoma revised. Report of two cases with immunohistochemical and electron microscopic study. Histogenetic considerations. *Neuropath Appl Neurobiol* 2000; **26**: 295-300.
 16. Port JD, Brat JD, Burger PC, Pomper MG. Astroblastoma: Radiographic-pathologic correlation and distinction from ependymoma. *Amer J Neuroradiol* 2000; **23**: 243-247.
 17. Shuangshoti S, Miphraphen W, Kanvisetsri S, Griffiths L, Navalitloha Y, Pornthanakasem W, Mutirangura A. Astroblastoma : Report of a case with microsatellite analysis. *Neuropathol* 2000; **20**: 228-232.
 18. Ortega-Aznar A, Romero-Vidal FJ, de la Tore, Castellvi J, Nogues P.

Neonatal tumors of the CNS: a report of 9 cases and a review. *Clin Neuropathol* 2001; **20**: 181-189.

19. Sugita Y, Terasaki M, Shigemori M, Morimatsu M, Honda E, Oshima Y. Astroblastoma with unusual signet-ring cell components: A case report and literature review. *Neuropathol* 2002; **22**: 200-205.
20. Rubinstein LJ, Herman MM. The astroblastoma and its possible cytogenic relationship to the tanycyte. An electron microscopic, immunohistochemical, tissue- and organ-culture study. *Acta Neuropathol* 1989; **78**: 472-483.
21. Nakazato Y, Sasaki A, Hirato J, Ishida Y. Immunohistochemical localization of neurofilament protein in neuronal degenerations. *Acta Neuropathol(Berl)* 1984;**64**:30-36
22. Bailey P, Bucy PC. Astroblastoma of the brain. *Acta Psychiat Neurol* 1930; **5**: 439-461.
23. Takeuchi H, Kubota T, Sato K, Llena JF, Hirano A. Epithelial differentiation and proliferative potential in spinal ependymomas. *J Neuro-Oncol* 2000; **58**: 13-19.
24. Dermietzel R, Traub O, Hwang TK, Beyer E, Bennett MVL, Spray DC, Willecke K. Differential expression of three gap junctions in developing and mature brain tissues. *Proc Natl Acad Sci USA* 1989; **86**: 10148-10152.
25. Zhang W, Couldwell WT, Simard MF, Song H, Lin JHC, Nedergaard M. Direct gap junction communication between malignant glioma cells and astrocytes. *Cancer Res* 1999; **59**: 1994-2003.
26. Nuber UA, Schäfer S, Stehr S, Rackwitz HR, Franke WW. Patterns of desmocollin synthesis in human epithelia: Immunolocalization of desmocollins 1 and 3 in special epithelia and in cultured cells. *Eur J Cell Bio* 1996; **71**: 1-13.
27. Takeuchi M. Cadherin cell adhesion receptors as a morphogenic regulator. *Science* 1991; **22**:1451-1455.

28. Cavallaro U, Schaffhauser B, Christofori G. Cadherin and the tumor progression : is it all a switch? *Cancer Letters* 2002; **176**: 123-128.
29. Bkakemore WF, Jolly RD. The subependymal plate and associated ependyma in the dog. An ultrastructural study. *J Neurocytol* 1972; **1**: 69-84.
30. Ugrumov MV, Miskevich MS. The adsorptive and transport capacity of tanycytes during the perinatal period of the rat. *Cell & Tissue Res* 1980; **211**: 493-501.
31. Flament-Durand J, Brion JP. Tanycytes: Morphology and Functions: A review. *Intern Rev Cytol* 1985; **96**: 121-155.
32. Horstmann E. Die Faserghlia des Selachiergehirns. *Z Zellforsch* 1954; **39**: 588-617.
33. Kawano N, Yagishita S, Tachibana S, Fujii K. Spinal tanycytic ependymomas. *Acta Neuropathol* 2001; **101**: 43-48
34. Langford LA, Barre GM. Tanycytic ependymoma. *Ultrastruct Pathol* 1997; **21**: 135-142
35. Sato K, Kubota T, Ishida M, Yoshida K, Takeuchi H, Handa Y. Immunohistochemical and ultrastructural study of chordoid glioma of the third ventricle: its tanycytic differentiation. *Acta Neuropathol* 2003; **106**: 176-180.
36. NG HK, Lo STH. Cytokeratin immunoreactivity in gliomas. *Histopathology* 1989; **14**: 359-368
37. Franke FE, Schachenmayr W, Osborn M, Altmannsberger M. Unexpected immunoreactivities of intermediate filament antibodies in human brain and brain tumors. *Amer J Pathol* 1991; **139**: 67-79.
38. Cosgrove MM, Rich KA, Kunin SA, Sherrod AE, Martin SE. Keratin intermediate filasment expression in astrocytic neoplasms: Analysis by immunochochemistry, western blot, and northern hybridization. *Modern Pathol* 1993; **6**: 342-347

Figure legends:

Fig.1A: Preoperative axial plain CT showing a high density large hemorrhagic mass.

Fig.1B.: Preoperative coronal contrast enhanced (CE) T1-weighted (W) MRI demonstrating a round circumscribed mass with mixed enhancement superficially located in the fronto-temporo-parietal lobe.

Fig.1C: Postoperative axial CE T1W-MRI 9 years after the first operation showing no tumor recurrence.

Fig.1D: Postoperative coronal CE T1W-MRI revealing a recurrent tumor 10 years after the first operation.

Fig.2A : Primary tumor shows a partially circumscribed mass consisting mainly of perivascular pseudorosettes. H & E

Fig.2B : Prominent sclerosing vessels with perivascular tumor cells (primary tumor). H & E

Fig.2C : The first recurrent tumor shows compactly arranged perivascular pseudorosettes composed of small tumor cells with round nuclei. A mitotic nucleus is seen (arrow). H & E

Fig.2D : Longitudinal section of perivascular tumor arrangement demonstrating a ribbon-like structure (the first recurrent tumor). H & E

Fig.2E : Immunoreactivity for GFAP expressing cells (primary tumor).

Fig.F: Cytokeratin (8 & 18Kd) immunoreactivity showing intensive positivity in the cytoplasm of tumor cells (the second recurrent tumor).

Fig.2G : Immunoreactivity for EMA is strongly positive along the cytoplasmic surface of tumor cells (the first recurrent tumor) .

Fig.2H : Connexin 26 immunoreactivity is extensively seen between the tumor cells (primary tumor) .

Fig.2I : Desmocollin 1 immunoreactivity is frequently positive between the tumor cells (the first recurrent tumor).

Fig.2J: Intensive immunoreactivity of N-cadherin along the tumor cell margin (primary tumor).

Fig.3 : Electron micrograph of an astroblastoma demonstrating remarkable perinuclear and intracytoplasmic tonofilament bundles. Desmosomes with tonofilaments are frequently seen. Intracytoplasmic organellae are well developed (primary tumor). X 10,000

Fig.4A: An irregular shaped nucleus with prominent nucleolus and rich microfibrils is shown. Junctional complexes are well developed. X 8,000

Fig.4B : Tumor cells project numerous microvilli and are connected by many junctional complexes. There are well-developed free ribosomes and mitochondria in the tumor cell cytoplasm (primary tumor). X 4,700

Fig.5A: Well-developed mature desmosomes with tonofilaments between the tumor cells (the first recurrent tumor). X 26,000

Fig.5B : Curious-shaped junctional complexes are frequently observed between the tumor cells (the first recurrent tumor). X 16,000

Fig.6A : Apical surface of the tumor cell projecting closely compact microvilli fanning from a narrow pedicle (the second recurrent tumor). X 10,000

Fig.6B : Long crowded microvilli projections resemble microrosettes in ependymoma, but there are no cilia in the tumor (the first recurrent tumor). X 13,000

Table 1 Antigens in used this study

Antigen	Source	Dilution
GFAP	DAKO(Z0334))	1: 2000
Vimentin	DAKO(M0725)	1:500
Keratin (56Kd & 64Kd)	DAKO(A0575)	1:1000
Cytokeratin (8Kd & 18Kd)	YLEM(MCC702)	1:200
EMA	DAKO(M0613)	1:200
Neurofilament (68Kd, 160Kd, 200Kd)	Nakazato(11)	1:800
r-Connexin 26	Zymed Lab Inc(Z.L.I) (71-0500)	1:500
m-Connexin 32	Z.L.I.(13-8200)	1:500
r-Connexin 43	Z.L.I.(71-0700)	1:500
m-Desmocollin 1	IMMUNO- Diagnostica(I.D)(65192)	1:500
m-Desmoglein 2	I.D.(65159)	1:500
m-Desmocollin 3	I.D.(65193)	1:500
h-E-cadherin	TAKARA(M106)	1:200
h-N-cadherin	Becton Dickinson	1:200
Ki-67	DAKO(M7240)	1:200

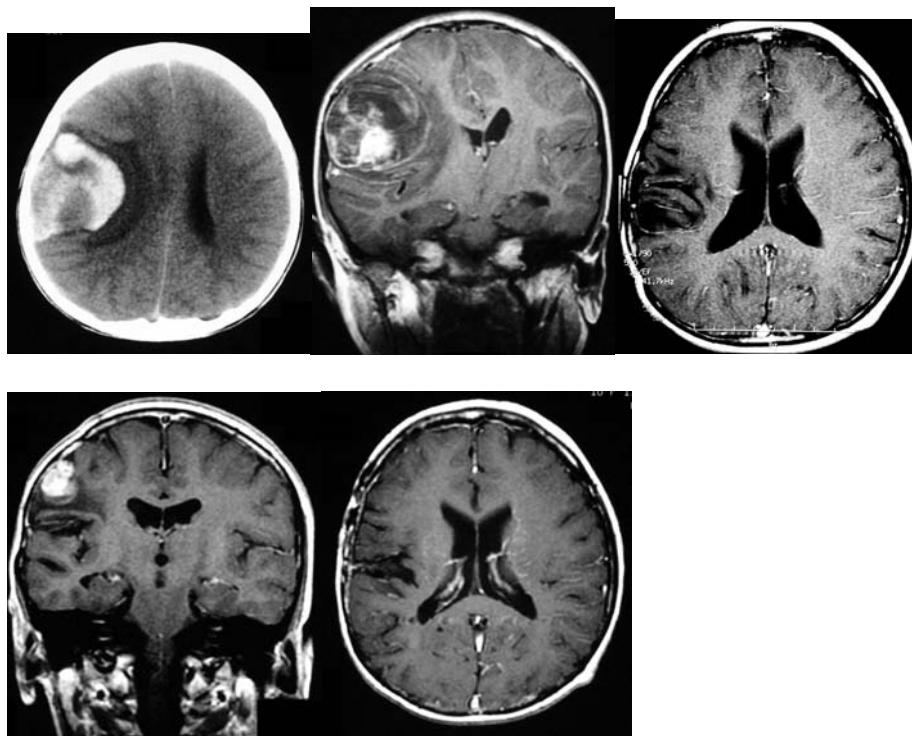
Abbreviations: GFAP:Glial Fibrillary Acidic Protein, EMA:Epithelial Membrane Antigen, m=mouse, h=human, r=rabbit

Table 2 Immunoreactivities of Primary and Recurrent Astroblastoma

Antibody	Primary Tumor	1 st Recurrent Tumor	2 nd Recurrent tumor
GFAP	+++	+++	+++
Vimentin	+++	+++	+++
Keratin (56Kd & 64Kd)	+	+	+
CAM5.2 (18Kd & 88Kd)	+	++	+++
EMA	+	++	+
Neurofilament (68Kd, 160Kd, 200Kd)	—	—	—
Connexin 26	++	+++	+++
Connexin 32	++	+++	+
Connexin 43	—	—	—
Desmocollin 1	++	+++	—
Desmoglein 2	—	—	—
Desmocollin 3	—	—	—
E-cadherin	+	+	—
N-cadherin	++	+++	++
Ki-67 LI	15.6%	25%	26.4%

Abbreviations: Staining Intensity : +++ ; strong, ++ ; moderate, + ; weak,
— ; Negative, LI ; Labeling Index

Fig.1



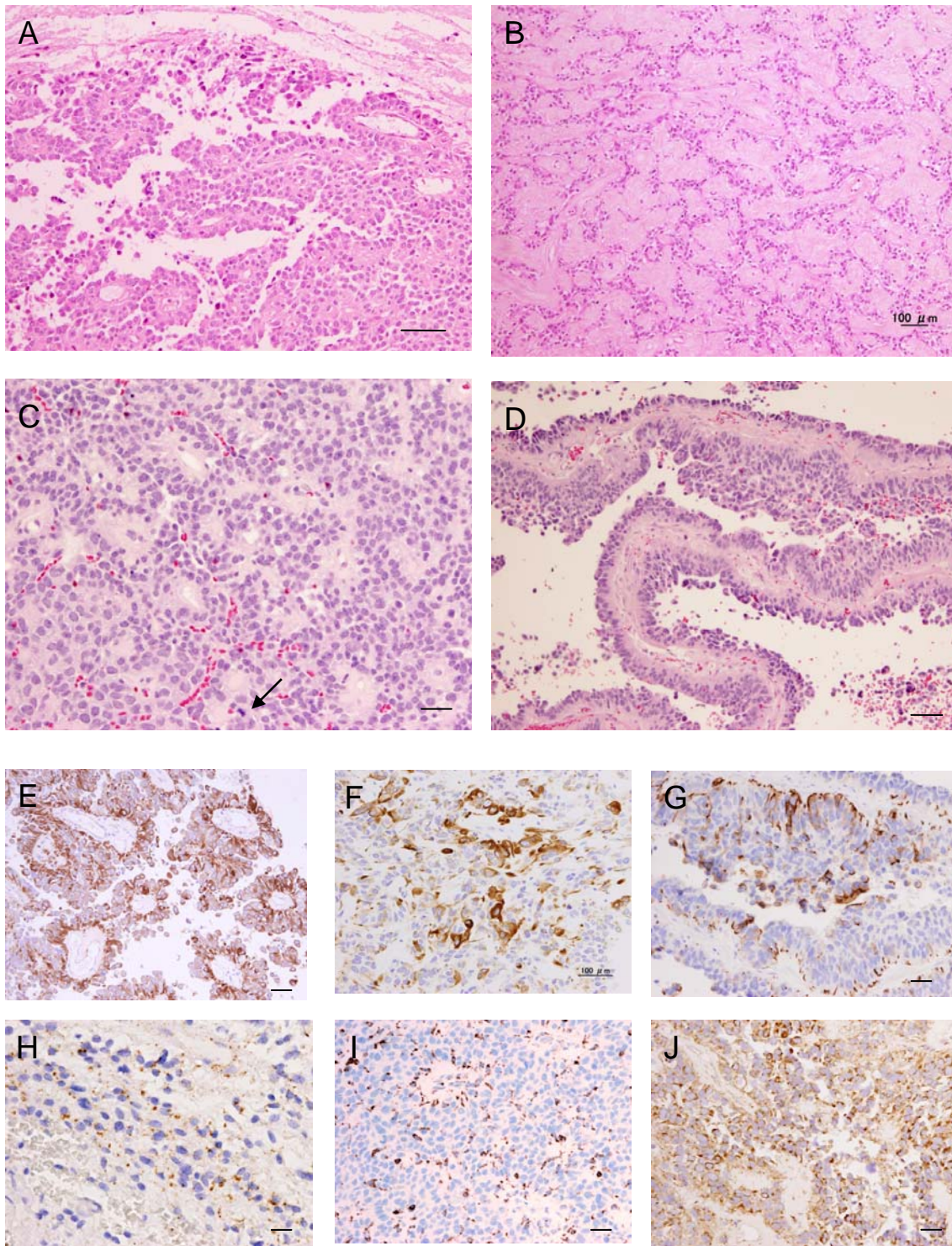


Fig.2

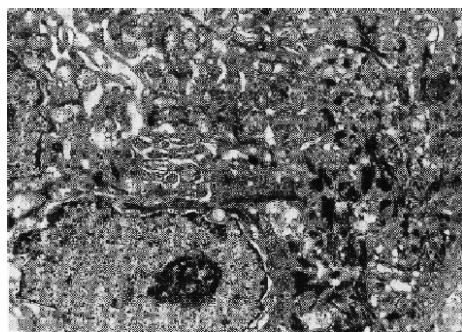


Fig.3

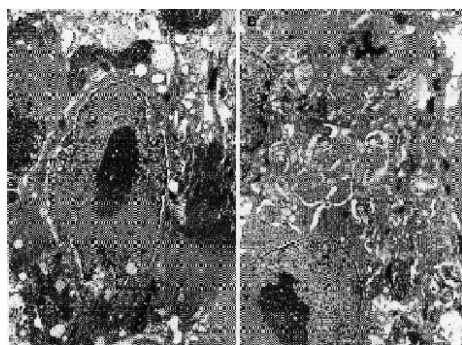


Fig.4

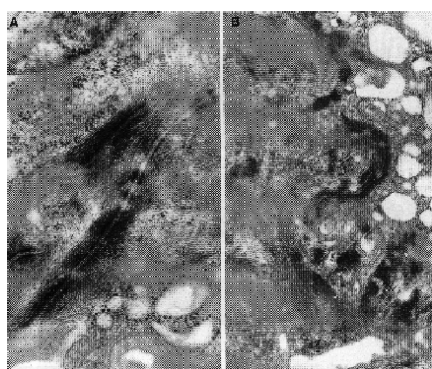


Fig.5

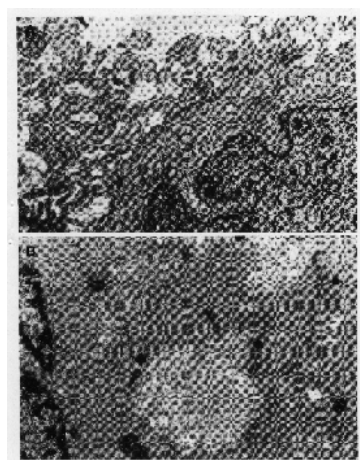


Fig.6